crystals

MDPI

Article

Growth of High Quality Al-Doped $CsLiB_6O_{10}$ Crystals Using Cs_2O-Li_2O-MoO_3 Fluxes

Xianchao Zhu [1,2], Heng Tu [1], Ying Zhao [1] and Zhanggui Hu [1,*]

[1] Key Lab of Functional Crystals and Laser Technology, Technical Institute of Physics and Chemistry, Chinese Academy of Sciences, Beijing 100190, China; zhuxianchao2008@163.com (X.Z.); tuheng@mail.ipc.ac.cn (H.T.); zhy@mail.ipc.ac.cn (Y.Z.)

[2] University of Chinese Academy of Sciences, Beijing 100049, China

* Correspondence: hu@mail.ipc.ac.cn

Academic Editor: Helmut Cölfen

Received: 31 January 2017; Accepted: 9 March 2017; Published: 13 March 2017

Abstract: High quality and large size Al-doped $CsLiB_6O_{10}$ (CLBO) single crystals have been successfully grown by top-seeded solution growth (TSSG) technique using Cs_2O–Li_2O–MoO_3 fluxes. The advantages of this newly developed flux system were investigated by viscosity measurements and growth experiments. Al-doped CLBO presents a very high transmittance in the visible region and the weak absorption values at 1064 nm along a and c axes are only 140 and 50 ppm/cm, respectively. The measured LIDT of Al-doped CLBO at λ = 1064 nm and τ = 5.0 ns is 5.10 GW/cm^2. Moreover, Al-doped CLBO exhibits an apparent enhancement of the hygroscopic nature in contrast with the undoped crystal as determined by the humidity experiments. Finally, a high fourth harmonic generation (FHG) conversion efficiency of 63% utilizing Al-doped CLBO has been achieved by a picosecond mode-locked Nd:YAG laser, the results also reveal that Al doping has no obvious impact on the FHG conversion efficiency.

Keywords: nonlinear optical crystals; top-seeded solution growth; CLBO; Al doping

1. Introduction

Nonlinear optical (NLO) crystal is one type of functional crystal that has been widely used in optical communication systems, industrial lasers, and microelectronic devices, owing to its various properties including electro-optical, nonlinear optical, photorefractive effects, etc. [1–3]. Recently, considerable research has been conducted on borate series nonlinear optical crystals for harmonic generation in high-power solid-state ultraviolet (UV) lasers due to their excellent properties such as relatively high tolerance to laser-induced damage, large nonlinear optical coefficients, moderate birefringence, and wide transparency range in the UV region. For instance, several borate crystals, such as β-BaB_2O_4 (BBO) [4], LiB_3O_5 (LBO) [5], CsB_3O_5 (CBO) [6], $CsLiB_6O_{10}$ (CLBO) [7,8], $KBe_2BO_3F_2$ (KBBF) [9], $YCa_4O(BO_3)_3$ (YCOB) [10], and $YA1_3(BO)_4$ (YAB) [11] have attracted a great deal of attention. Among these crystals, CLBO is a newly developed borate crystal and has been successfully applied for the fourth and fifth-harmonic generation of a Nd:YAG laser [12,13]. After firstly reported by researchers in 1995 [7,8,14–16], CLBO is considered as a highly promising NLO crystal due to its small walk-off angle and relatively large phase-matching angular, spectral, and temperature acceptance bandwidths compared with other borate NLO crystals [12,17]. Additionally, in comparison with other commercially available NLO crystals such as BBO and LBO, CLBO possesses incomparable advantages, since it can be easily grown from congruent or near-congruent melts at extremely fast growth rate by top-seeded solution growth (TSSG) method [16,18].

Since CLBO melts congruently at 848 °C, many growth techniques could be utilized to grow CLBO single crystals. The TSSG method has been commonly used to grow CLBO crystals. Currently,

a self-flux poor in B_2O_3 is extensively employed to grow CLBO crystal with the purpose of reducing the viscosity of stoichiometric melt [14,19]. Meanwhile, increasing attention has been paid to obtaining uniform supersaturation during crystal growth by means of solution stirring or crucible rotation technique [19–21]. Kyropoulos and Czochralski methods have also been applied to grow large size CLBO by many researchers [18,22,23].

Despite having favorable growth habit, the major challenge to the practical application of CLBO is its highly hygroscopic behavior, which can result in the deterioration of the crystal quality and ultimately lead to cracking [24,25]. To date, many authors have devoted their efforts to investigating the hygroscopic nature and cracking mechanism of CLBO crystal [18,26–29], as well as the influence of hygroscopy on the nonlinear optical properties [25]. On one hand, previous researchers stated that water molecules attacked CLBO crystal along the a axis much more easily than along the c axis because of relatively large channels that exist parallel to the a axis [26], and it was also observed that water molecules were incorporated into the Cs defect [23]. Additionally, researchers reported that surface hydration rate mainly depends on the humidity of the environment, and it was concluded that hydration occurred at a relatively faster rate at higher humidity (>45%), and eventually resulted in crystal cracking and the formation of $Cs_2B_{10}O_{16}\cdot 8H_2O$ [18,26,29]. On the other hand, many researchers pointed out that surface hydration had an adverse effect on the optical properties, such as refractive index distortions and decline in bulk LIDT and UV transmittance [30–32].

Thus, efforts in developing effective techniques to solve the hydration problem are very important. During the last few years there has been considerable progress in the practical application of CLBO. According to earlier studies, water impurity can be effectively eliminated by long time heat treatment of CLBO crystal at 150–160 °C [25,31,32], whereas it is inconvenient in practical application. Recent studies have revealed that surface degradation of CLBO can be significantly suppressed by Al doping [33]. In recent years, self-flux has been widely utilized to grow Al-doped CLBO crystals. However, it was very difficult to grow high-quality Al-doped CLBO crystals because of the relatively high viscosity and instability of self-flux system, which can lead to the generation of crystal defects such as inclusions and decrease laser-induced damage threshold and transmittance. As was previously mentioned, MoO_3 flux exhibits outstanding properties and has been successfully applied to grow many borate crystals, such as LBO [34], CBO [35], and YAB [36], etc. It is generally considered that MoO_3 can effectively cause structural changes in the boron-oxygen network, which leads to a weaker connectivity in the boron-oxygen network and thus drastically reducing the viscosity of the growth system [37]. In 1999, Pylneva [38] et al. firstly reported the crystallization region in Cs_2O–Li_2O–B_2O_3–MoO_3 system and obtained an undoped CLBO crystal with size of $60 \times 40 \times 20$ mm^3, but the viscosity of this system has not been measured. Moreover, they also briefly described the growth of Al-doped CLBO crystal, but there was no detailed crystal growth investigation or relevant properties characterization. Up to now in the literature, there are no other papers related to the growth of CLBO using MoO_3 flux. Therefore, this paper is aimed at attempting to grow large size and high quality Al-doped CLBO crystals using Cs_2O–Li_2O–MoO_3 fluxes.

In the present study, high quality undoped and Al-doped CLBO crystals were successfully grown from optimized Cs_2O–Li_2O–MoO_3 flux system by TSSG method. We carried out a detailed investigation of crystal growth as well as the viscosity measurement of this flux system. The as-grown crystals were characterized by powder X-ray diffraction, transmittance spectra, optical weak absorption, and LIDT. Furthermore, the effect of Al doping on the hygroscopic behavior and fourth harmonic generation (FHG) conversion efficiency of CLBO crystal were investigated by humidity experiments and laser output performance, respectively.

2. Experimental

2.1. Crystal Growth

The starting material was synthesized from high purity reagents Cs_2CO_3, Li_2CO_3, H_3BO_3, and MoO_3 at an appropriate ratio with the addition of a certain amount of Al_2O_3. After being accurately weighed and mixed homogeneously, it was then melted in a Ø 90 × 80 mm^3 platinum crucible at 900 °C in several batches. The crucible was placed in a three-zone resistance furnace controlled by a programmable Eurotherm (model 818) temperature controller. Then, the mixture was heated to approximately 50 °C above the melting point, followed by stirring with a platinum stirrer for 48 h to enable the solution to melt completely and mix uniformly. The saturation temperature was precisely determined by seeding measurements method, and the suitable vertical temperature gradient was about 1 °C/6 cm. A high quality [001] oriented seed crystal was slowly introduced into the solution surface at a temperature of 1 °C higher than the saturation temperature and maintained at this temperature for half an hour. The growth rate was carried out at a very slow cooling rate in the range of 0.05–0.1 °C/day in the initial stage. The growing crystal was rotated at a rate of 20–50 rpm with the rotation direction inverted every 2 min. After the growth finished, the crystal was carefully drawn out of the solution surface and cooled to room temperature at a rate of 5–10 °C/h.

2.2. Characterization

The viscosity of growth solution was measured by a DVII + Pro viscometer (Brookfield Co., Middleboro, MA, USA). Powder X-ray diffraction (XRD) measurement was verified by a computer-automated Bruker D8 Focus diffractometer equipped with Cu Kα radiation (λ = 1.54056 Å). The as-grown Al-doped crystals were analyzed by inductively coupled plasma mass spectrometry (ICP-MS) for the determination of Al^{3+} concentrations. The transmission spectrum was recorded using a Perkin-Elmer Lambda 900 UV-Vis-near-infrared (NIR) spectrophotometer in the wavelength range of 185–1800 nm at room temperature. Optical weak absorption testing at 1064 nm was performed by the photo-thermal common path interferometer (PCI) method. The laser-induced damage threshold of the crystal was determined by a Continuum Surelite II pulsed Nd:YAG laser system. The surface etching morphology of CLBO crystal induced by humidity was observed on the (001) planes using an optical microscope (Nikon SMZ 745T, Nikon Co., Kanagawa, Japan). In the laser output experiment, a 532 nm Nd:YAG laser was utilized as the fundamental source, and then doubled to 266 nm for the measurement of conversion efficiency.

3. Results and Discussion

3.1. Crystal Growth and Viscosity Measurement

As previously reported [38], the molar ratio of Cs_2O:Li_2O:B_2O_3:MoO_3 for CLBO crystal growth was in the range of 1:(1.0–1.5):(3.0–6.0):(0.5–1.0). According to our growth results of various solution compositions, we determined that the appropriate molar ratio was 1:1:3:1. After the appropriate molar ratio of this flux system was identified, undoped and 2.5%–10% Al-doped CLBO were successfully grown with growth duration of 30–40 days. The as-grown undoped and Al-doped crystals were free from visible cracks and inclusions, as shown in Figure 1. The detailed growth conditions and results are summarized in Table 1. It is clear that the cooling range varies from 3.2 to 4.1 °C in this flux system, apparently wider than that of self-flux system (1–1.5 °C) [14,19], indicating that this flux system is conducive to the growth of large size crystals.

The volatility and the viscosity—two crucial parameters during crystal growth—both depend on solution temperature and composition. Low volatility and viscosity are beneficial to mass and heat transfer as well as to maintain the stability of solution components. Hence, a flux system with low volatility and viscosity is vitally important to grow high quality crystal.

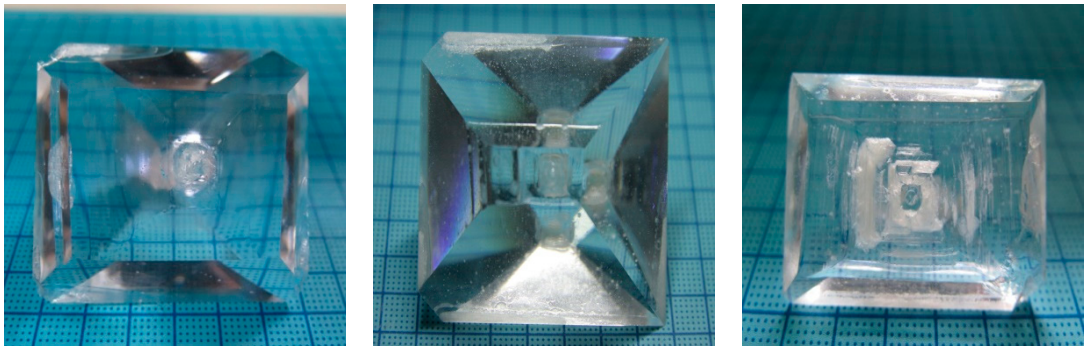

(**a**) (**b**) (**c**)

Figure 1. Photos of as-grown crystals: (**a**) undoped CLBO; (**b**) 2.5% Al-doped CLBO; (**c**) 5% Al-doped CLBO.

Table 1. The detailed growth conditions and results of undoped and Al-doped $CsLiB_6O_{10}$ (CLBO) crystals.

Al Doping Concentration	Al:Li (Molar Ratio)	Saturation Temperature (°C)	Cooling Range (°C)	Size (mm^3), Weight (g)	Inclusions
undoped	0	800	3.4	61 × 59 × 35, 125	free
2.5% Al-doped	2.5:97.5	802	4.1	68 × 59 × 47, 170	free
5% Al-doped	5:95	808	3.3	54 × 35 × 25, 64	free
10% Al-doped	10:90	811	3.2	50 × 49 × 26, 61	almost free

Table 1 shows that the measured saturation temperature was in the range of 800–811 °C, which was remarkably lower than that of self-flux system (837–844 °C) [39]. Consequently, this flux system can reduce volatility so as to avoid component deviation caused by the relatively high evaporation of Cs. In the case of Al-doped CLBO grown from self-flux system, it is difficult to accurately determine saturation temperature due to the relatively great fluctuation of saturation temperature induced by volatiles. Additionally, the seed crystal can be easily etched by the volatiles from the solution, resulting in the growing crystal falling. However, in our growth experiments utilizing MoO_3 flux, these disadvantages could be effectively eliminated. The viscosity of a Cs_2O–Li_2O–B_2O_3–MoO_3 system in the temperature range of 780–880 °C has been determined by the present authors for the first time, and the results are illustrated in Figure 2. As can be seen from the figure, the viscosity increases gradually with the increase of Al doping concentration at the same temperature. Or rather, the viscosity increases rapidly from 198.4 to 239.5 cP with increasing Al doping concentration only from 2.5% to 5% at 800 °C, but it changes slightly with Al doping concentration in range of 0%–2.5% and 5%–10%. The viscosities of undoped, 2.5%, 5%, and 10% Al-doped CLBO growth solutions at their corresponding saturation temperature are 182.5, 198.4, 205.3, and 209.8 cP, respectively. Obviously, there is a tremendous decrease in viscosity compared with self-flux system (the viscosity beyond 1000 cP) [40], which often inevitably leads to low growth repeatability and the formation of inclusions in crystal. The above results confirm that the introduction of MoO_3 can enormously reduce the viscosity of the growth solution. Thus, the Cs_2O–Li_2O–B_2O_3–MoO_3 system has a great advantage over the Cs_2O–Li_2O–B_2O_3 system in that it possesses a clearly lower volatility and a significantly lower viscosity.

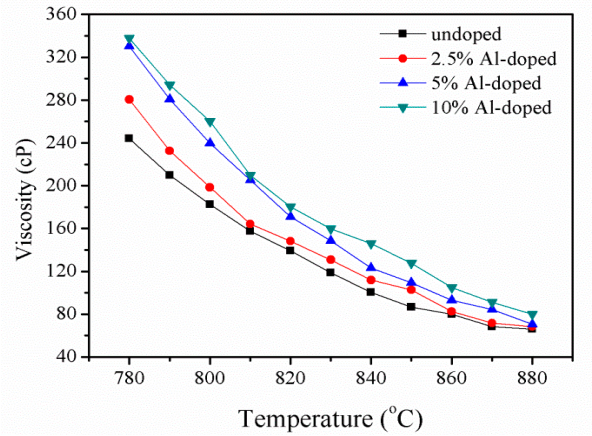

Figure 2. Viscosities of CLBO growth solutions with different Al doping concentrations.

3.2. XRD and ICP Analysis

The powder X-ray diffraction (XRD) measurement was performed to verify the structure of as-grown Al-doped crystals. As displayed in Figure 3, we found that the positions and intensities of main diffraction peaks are well in accordance with these of undoped CLBO crystal. The results confirm that Al doping do not change the essential structure of CLBO.

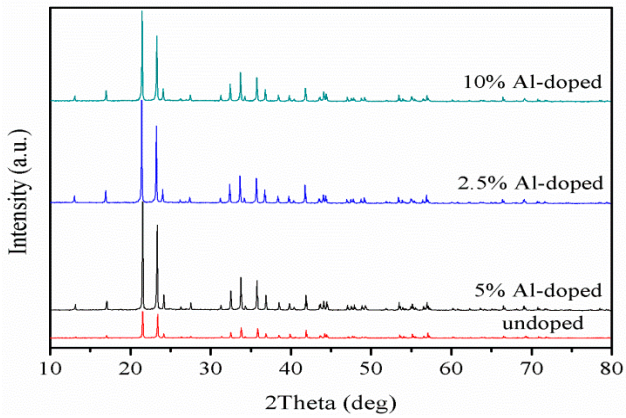

Figure 3. XRD patterns of undoped and Al-doped CLBO crystals.

In order to determine the effective Al^{3+} segregation coefficient, ICP analysis was carried out to measure the Al^{3+} concentration in the crystal. The effective segregation coefficient K can be calculated by the following equation: $k = C_s/C_0$, where C_s and C_0 correspond to Al^{3+} concentration in the crystal and Al^{3+} concentration in the growth solution, respectively. Based on the measured Al^{3+} concentration in the as-grown crystal, the calculated effective Al^{3+} segregation coefficients of 2.5%, 5%, and 10% Al-doped CLBO crystals are 0.028, 0.034, and 0.031, respectively, which are slightly higher than those of previous study [39].

3.3. Transmission Spectrum

For investigation of Al doping on the transmittance, the as-grown crystals were cut along (001) wafer and optically polished to about 1 mm thickness for spectrum measurement. The transmission spectrum of undoped and Al-doped CLBO crystals ranging from 185 to 1800 nm are presented in Figure 4. As is evident from Figure 4, both undoped and Al-doped crystals exhibit extremely high transmittance and exceed 92%. Moreover, there was no absorption band in the range of 200–380 nm, demonstrating that Mo ion did not crystallize into the crystal, and thus the ultraviolet cutoff wavelength

could not be shifted [35]. Consequently, it can be concluded that as-grown crystals present excellent optical quality and Al doping has no adverse effect on the transmittance.

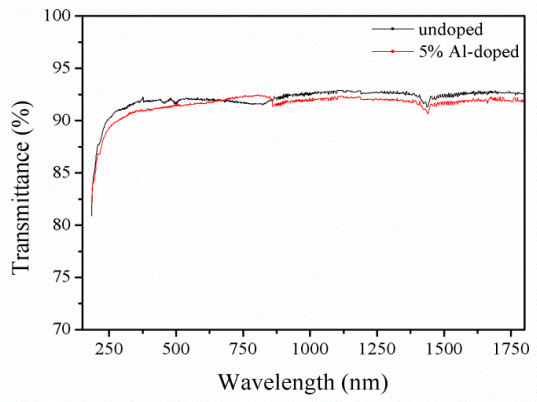

Figure 4. Transmission spectrum of undoped and Al-doped CLBO crystals.

3.4. Laser-Induced Damage Threshold

Laser-induced damage is one of the major limitations associated with the development of high-power solid-state lasers, because it can seriously restrict the available input power. Bulk laser-induced damage is mainly related to crystal quality, so we measured the bulk LIDT of as-grown crystal for the purpose of evaluating its prospect in practical applications. The CLBO crystal sample with dimensions of $5 \times 5 \times 5$ mm^3 was employed and two (001) faces were optically polished. The bulk LIDT was tested by means of the 1-on-1 test procedure using a Q-switched Nd:YAG laser (1064 nm) operating in a longitudinal single mode. The pulse repetition rate and pulse duration were 1 kHz and 5 ns, respectively. During the measurement, ten sites were chosen as test points at each pulse fluence, and laser-induced damage was confirmed to have occurred by visual observation of a laser spark. The pulse fluence which causes the corresponding damage probability of 0% is defined as the laser-induced damage threshold of the sample.

Figure 5 shows the measured damage probability of undoped and Al-doped CLBO crystals. The results show that the LIDT of undoped and Al-doped CLBO crystals along the c axis are 33.98 J/cm^2 (6.80 GW/cm^2) and 25.48 J/cm^2 (5.10 GW/cm^2), respectively. The LIDT of newly-grown undoped CLBO significantly exceed that of conventional undoped CLBO (5.72 GW/cm^2 at 1064 nm along the c axis) [15]; the enhancement of LIDT may be attributed to high crystallinity and low dislocation density of crystal [19,20,41]. Hence, the results further prove the high quality of as-grown crystals and their promising applications in high-power solid-state lasers.

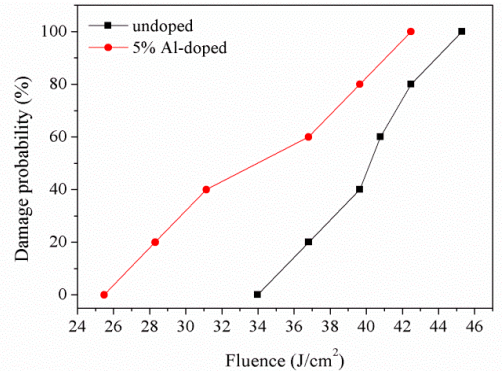

Figure 5. Bulk LIDT of undoped and Al-doped CLBO crystals.

3.5. Optical Weak Absorption

The PCI system is a precise weak absorption measurement apparatus based on surface thermal lensing technique. The probe beam crosses the pump beam at a certain angle. As the crystal sample is irradiated by a pump beam, the refractive index change can occur in the heated area. Accordingly, the probe beam suffered phase distortion in this area induced by common-path point diffraction interference. The perceived phase distortion signals of the probe beam are collected by a photodetector behind an aperture, and then are accurately processed by the lock-in amplifier and transmitted to the computer. Samples with size of $5 \times 5 \times 5$ mm^3 were optically polished for this measurement.

The optical weak absorption curves of undoped and Al-doped CLBO crystals at the critical wavelength of 1064 nm were obtained, as presented in Figures 6 and 7, respectively. The two highest peaks are regarded as the weak absorption of two end surfaces of the crystal, while the stable area between the two peaks represents the measured bulk weak absorption of the crystal. As seen from the two figures, the weak absorption values of undoped CLBO crystal along a and c directions were only 80 and 50 ppm/cm, respectively, while the weak absorption values of Al-doped CLBO crystal along a and c directions were approximately 140 and 50 ppm/cm, respectively. The measured weak absorption values are dramatically lower compared to previous investigation (600 ppm/cm for a direction and 150 ppm/cm for c direction) [42], as listed in Table 2. To our knowledge, the measured weak absorption values in the present work are by far the minimum levels reported in articles. Since the weak absorption values are closely correlated with the optical quality of the crystal, the newly grown crystals possess outstanding optical quality.

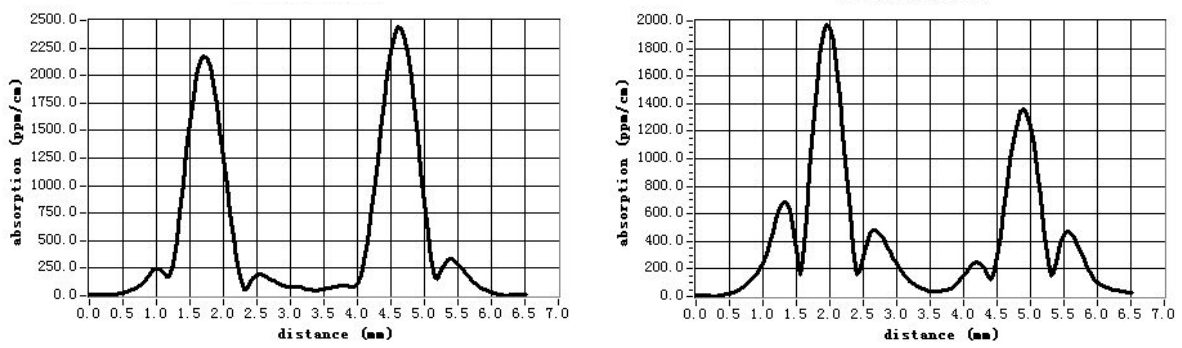

Figure 6. Weak absorption curves of undoped CLBO crystal along (**left**) a and (**right**) c directions.

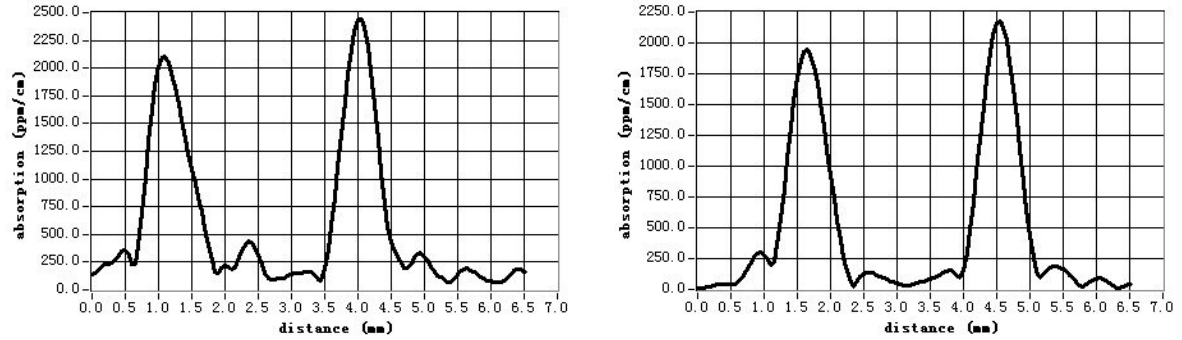

Figure 7. Weak absorption curves of 5% Al-doped CLBO crystal along (**left**) a and (**right**) c directions.

Table 2. Weak absorption values of CLBO crystals.

CLBO Crystals	Weak Absorption Value at 1064 nm/ppm·cm^{-1}	
	[100] Direction	[001] Direction
Undoped CLBO	80	50
5% Al-doped CLBO	140	50
Conventional CLBO [42]	600	150

3.6. Humidity Experiment

In order to investigate the influence of Al doping on the hygroscopic behavior of CLBO crystal, a humidity experiment was conducted at a constant temperature in a humidity chamber. Two optically polished samples with dimensions of 4 × 4 × 3 mm^3—namely, A (undoped CLBO crystal) and B (5% Al-doped CLBO crystal)—were kept in the program-controlled chamber at relative humidity of 60% and temperature of 25 °C for different durations. The surface micrographs of the (001) plane are given in Figure 8 (under an optical microscope with 100 magnification). From Figure 8, some regular etch pits can be clearly observed on the edges of (001) plane in sample A with an increase in duration time from 0 to 1200 h. In contrast, there were no observable etch pits in sample B, even over a period of 50 days. The results demonstrate that Al doping could substantially improve the hygroscopic nature of CLBO.

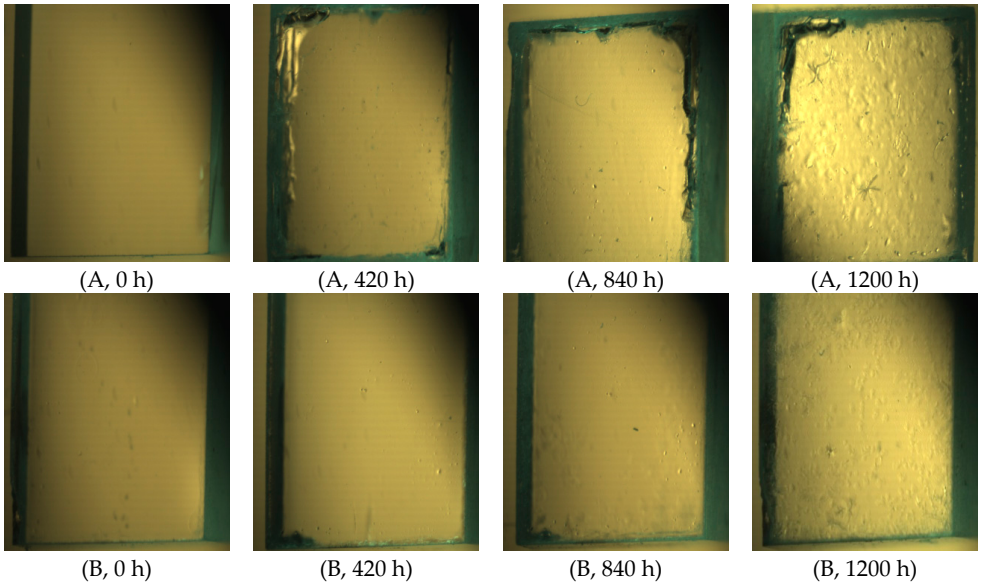

Figure 8. Microphotographs of the (001) plane in (**A**) undoped and (**B**) Al-doped CLBO crystals for different durations.

3.7. 266 nm UV Laser Conversion Efficiency

A picosecond mode-locked Nd:YAG laser (pulse width: 25 ps, pulse repetition frequency: 10 Hz) was employed as the fundamental light source for the laser output and fourth harmonic generation (FHG) conversion efficiency measurements. Samples of uncoated and optically polished undoped and Al-doped CLBO crystals with dimension of 3 × 3 × 10 mm^3 were cut along the angles of (θ, ϕ) = (61.6°, 45°) and $\theta_{Brewster}$ = 56.3° according to type-I phase matching direction. Figure 9 displays the conversion efficiency of the 266 nm radiation as a function of 532 nm input peak power density. Remarkably, the FHG conversion efficiency from 532 nm to 266 nm of CLBO increases gradually with increasing the 532 nm input peak power density. The maximum conversion efficiencies of undoped and Al-doped CLBO crystals can reach 65% and 63% at their corresponding peak power density of 325

MW/cm^2, respectively. Despite the FHG conversion efficiency of Al-doped CLBO crystal is slightly lower than that of undoped CLBO crystal, the difference between them being very small. The decrease of conversion efficiency may be connected with the reduction of the crystalline perfection due to Al doping [43]. The results illustrate that Al doping has no obvious influence on the FHG conversion efficiency of CLBO.

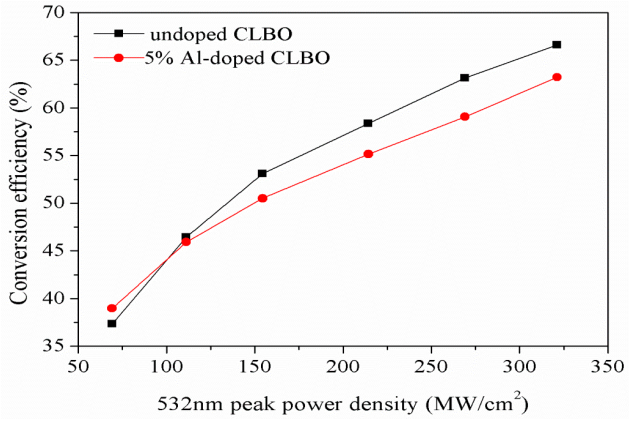

Figure 9. Peak power density dependence at 532 nm of fourth harmonic generation (FHG) conversion efficiency of CLBO crystals.

4. Conclusions

In summary, undoped and Al-doped CLBO crystals free from inclusions were successfully grown using the newly developed Cs_2O–Li_2O–MoO_3 fluxes. The Cs_2O–Li_2O–B_2O_3–MoO_3 system could drastically lower the viscosity of the growth solution compared to that of extensively used self-flux system. The as-grown crystals exhibited excellent quality. The measured weak absorption values of undoped and Al-doped CLBO were remarkably smaller than previous studies. The LIDT of undoped CLBO came up to 6.80 GW/cm^2—19% higher than that of conventional undoped CLBO. Our results further illustrate that Al doping can significantly enhance the resistance of CLBO to water. The undoped and Al-doped CLBO with FHG conversion efficiencies greater than 63% have been realized, and Al doping has a weak influence on FHG conversion efficiency. Therefore, the newly grown Al-doped CLBO crystal has been demonstrated to be a highly promising NLO crystal for UV light generation.

Acknowledgments: This work was supported by National Key R&D program of China (No. 2016YFB0402100).

Author Contributions: Xianchao Zhu finished the experiment and wrote this manuscript; Heng Tu helped perform the analysis with constructive discussions; Ying Zhao provided materials and analysis tools; Zhanggui Hu designed the experiments and revised the manuscript. All authors read and approved the manuscript.

Conflicts of Interest: The authors declare no conflict of interest.

References

1. Arizmendi, L. Photonic applications of lithium niobate crystals. *Phys. Status Solidi A.* **2004**, *201*, 253–283. [CrossRef]
2. Wang, G.; Liu, J.; Liu, S.; Liu, M.; Liu, S.; Li, L. Short pulse duration of a 355-nm laser by extracavity sum-frequency mixing with a LiB_3O_5 (LBO) crystal. *Laser Phys. Lett.* **2008**, *5*, 506–509. [CrossRef]
3. Anisa, M.; Muleya, G.G.; Hakeem, A.; Shirsat, M.D.; Hussaini, S.S. Exploring the influence of carboxylic acids on nonlinear optical (NLO) and dielectric properties of KDP crystal for applications of NLO facilitated photonic devices. *Opt. Mater.* **2015**, *46*, 517–521. [CrossRef]
4. Chen, C.T.; Fan, Y.X.; Eckardt, R.C.; Byeret, R.L. Recent Developments in Barium Borate. *Proc. SPIE* **1987**, *0681*, 12–17.

5. Chen, C.T.; Wu, Y.C.; Jiang, A.D.; Wu, B.C.; You, G.M.; Li, R.K.; Lin, S.J. New nonlinear-optical crystal: LiB_3O_5. *J. Opt. Soc. Am. B.* **1989**, *6*, 616–621. [CrossRef]
6. Wu, Y.C.; Sasaki, T.; Nakai, S.; Yokotani, A.; Tang, H.G.; Chen, C.T. CsB_3O_5: A new nonlinear optical crystal. *Appl. Phys. Lett.* **1993**, *62*, 2614–2615. [CrossRef]
7. Sasaki, T.; Mori, Y.; Kuroda, I.; Nakajima, S.; Yamaguchi, K.; Watanabe, S.; Nakai, S. Caesium Lithium Borate: a New Nonlinear Optical Crystal. *Acta Crystallogr. Sect. C Struct. Chem.* **1995**, *51*, 2222–2224. [CrossRef]
8. Mori, Y.; Kuroda, I.; Nakajima, S.; Sasaki, T.; Nakai, S. New nonlinear optical crystal: Cesium lithium borate. *Appl. Phys. Lett.* **1995**, *67*, 1818–1820. [CrossRef]
9. Mei, L.F.; Wang, Y.B.; Chen, C.T.; Wu, B.C. Nonlinear optical materials based on $MBe_2BO_3F_2$ (M = Na, K). *J. Appl. Phys.* **1993**, *74*, 7014–7015. [CrossRef]
10. Fei, Y.T.; Chai, B.H.T.; Ebbers, C.A.; Liao, Z.M.; Schaffers, K.I; Thelin, P. Large-aperture YCOB crystal growth for frequency conversion in the high average power laser system. *J. Cryst. Growth* **2006**, *290*, 301–306. [CrossRef]
11. Yu, X.S.; Yue, Y.C.; Yao, J.Y.; Hu, Z.G. $YAl_3(BO_3)_4$: Crystal growth and characterization. *J. Cryst. Growth* **2010**, *312*, 3029–3033. [CrossRef]
12. Wang, G.L.; Geng, A.C.; Bo, Y.; Li, H.Q.; Sun, Z.P.; Bi, Y.; Cui, D.F.; Xu, Z.Y.; Yuan, X.; Wang, X.Q.; et al. 28.4 W 266 nm ultraviolet-beam generation by fourth-harmonic generation of an all-solid-state laser. *Opt. Commun.* **2006**, *259*, 820–822. [CrossRef]
13. Yap, Y.K.; Inagaki, M.; Nakajima, S.; Mori, Y.; Sasaki, T. High-power fourth- and fifth-harmonic generation of a Nd:YAG laser by means of a $CsLiB_6O_{10}$. *Opt. Lett.* **1996**, *21*, 1348–1350. [CrossRef] [PubMed]
14. Mori, Y.; Kuroda, I.; Nakajima, S.; Taguchi, A.; Sasaki, T.; Nakai, S. Growth of a nonlinear optical crystal: Cesium lithium borate. *J. Cryst. Growth* **1995**, *156*, 307–309. [CrossRef]
15. Mori, Y.; Kuroda, I.; Nakajima, S.; Sasaki, T.; Nakai, S. Nonlinear Optical Properties of Cesium Lithium Borate. *Jpn. J. Appl. Phys.* **1995**, *34*, 296–298. [CrossRef]
16. Sasaki, T.; Kuroda, I.; Nakajima, S.; Watanabe, S.; Mori, Y.; Nakai, S. New Nonlinear Optical Crystal Cesium Lithium Borate. *Proc. Adv. Solid State Lasers Conf.* **1995**, *24*, 91–95.
17. Mori, Y.; Yap, Y.K.; Inagaki, M.; Nakajima, S.; Taguchi, A.; Zhou, W.L.; Sasaki, T. High efficiency UV light generation by CLBO. In Proceedings of the Advanced Solid State Lasers, San Francisco, CA, USA, 31 January 1996; pp. 341–345.
18. Yuan, X.; Shen, G.Q.; Wang, X.Q.; Shen, D.Z.; Wang, G.L.; Xu, Z.Y. Growth and characterization of large CLBO crystals. *J. Cryst. Growth* **2006**, *293*, 97–101. [CrossRef]
19. Sasaki, T.; Mori, Y.; Yoshimura, M. Progress in the growth of a $CsLiB_6O_{10}$ crystal and its application to ultraviolet light generation. *Opt. Mater.* **2003**, *23*, 343–351. [CrossRef]
20. Ono, R.; Kamimura, T.; Fukumoto, S.; Yap, Y.K.; Yoshimura, M.; Mori, Y.; Sasakia, T.; Yoshida, K. Effect of crystallinity on the bulk laser damage and UV absorption of CLBO crystals. *J. Cryst. Growth* **2002**, *237–239*, 645–648. [CrossRef]
21. Reddy, B.; Elizabeth, S.; Bhat, H.L.; Karnal, A.K. Development of a versatile high temperature top seeded solution growth unit for growing cesium lithium borate crystals. *Rev. Sci. Instrum.* **2009**, *80*, 013908. [CrossRef] [PubMed]
22. Hartmann, E.; Péter, Á; Lengyel, K.; Kovács, L. Effect of melt composition on the electrical conductivity and IR absorption of $CsLiB_6O_{10}$ crystals. *Cryst. Res. Technol.* **2003**, *3–5*, 331–335. [CrossRef]
23. Isaenko, L.; Vasilyeva, I.; Merkulov, A.; Tomilenko, A.; Bogdanova, I.; Malakhov, V.; Drebushchak, V. $CsLiB_6O_{10}$ crystals with Cs deficit: Structure and properties. *J. Cryst. Growth* **2005**, *282*, 407–413. [CrossRef]
24. Kovács, L.; Lengyel, K.; Péter, Á.; Polgár, K.; Beran, A. IR absorption spectroscopy of water in $CsLiB_6O_{10}$ crystals. *Opt. Mater.* **2003**, *24*, 457–463.
25. Yap, Y.K.; Inoue, T.; Sakai, H.; Kagebayashi, Y.; Mori, Y.; Sasaki, T.; Deki, K.; Horiguchi, M. Long-term operation of $CsLiB_6O_{10}$ at elevated crystal temperature. *Opt. Lett.* **1998**, *23*, 34–36. [CrossRef] [PubMed]
26. Pan, F.; Wang, X.Q.; Shen, G.Q.; Shen, D.Z. Cracking mechanism in CLBO crystals at room temperature. *J. Cryst. Growth* **2002**, *241*, 129–134. [CrossRef]
27. Ryu, G.; Yoon, C.S.; Han, T.P.J.; Gallagher, H.G. Growth and characterisation of $CsLiB_6O_{10}$ (CLBO) crystals. *J. Cryst. Growth* **1998**, *191*, 492–500. [CrossRef]
28. Taguchi, A.; Miyamoto, A.; Mori, Y.; Haramura, S.; Inoue, T.; Nishijima, K.; Kagebayashi, Y.; Sakai, H.; Yap, Y.K.; Sasaki, T. Effect of the moisture on CLBO. *OSA TOPS Adv. Solid State Lasers* **1997**, *10*, 19–23.

29. Seryotkin, Y.V.; Fomina, E.A.; Isaenko, L.I. Humidity effect on hydration of $CsLiB_6O_{10}$ nonlinear optical crystal: X-ray diffraction study. *Opt. Mater.* **2013**, *35*, 1646–1651. [CrossRef]
30. Takachiho, K.; Yoshimura, M.; Takahashi, Y.; Imade, M.; Sasaki, T.; Mori, Y. Ultraviolet laser-induced degradation of $CsLiB_6O_{10}$ and β-BaB_2O_4. *Opt. Mater. Express* **2014**, *4*, 559–567. [CrossRef]
31. Kawamura, T.; Yoshimura, M.; Honda, Y.; Nishioka, M.; Shimizu, Y.; Kitaoka, Y.; Mori, Y.; Sasaki, T. Effect of water impurity in $CsLiB_6O_{10}$ crystals on bulk laser-induced damage threshold and transmittance in the ultraviolet region. *Appl. Opt.* **2009**, *48*, 1658–1662. [CrossRef] [PubMed]
32. Nishioka, M.; Kanoh, A.; Yoshimura, M.; Mori, Y.; Sasaki, T.; Katsura, T.; Kojima, T.; Nishimae, J. Improvement in UV Optical Properties of $CsLiB_6O_{10}$ by Reducing Water Molecules in the Crystal. *Jpn. J. Appl. Phys.* **2005**, *44*, 699–700. [CrossRef]
33. Mori, Y.; Sasaki, T. $CsLiB_6O_{10}$ crystal: Growth and properties. *Proc. SPIE* **1996**, *2700*, 20–27.
34. Hu, Z.G.; Zhao, Y.; Yue, Y.C.; Yu, X.S. Large LBO crystal growth at 2 kg-level. *J. Cryst. Growth* **2011**, *335*, 133–137. [CrossRef]
35. Liu, S.S.; Zhang, G.C.; Li, X.M.; Yang, F.; Bo, Y.; Fu, P.Z.; Wu, Y.C. Growth and characterization of CsB_3O_5 crystals without scattering centers. *CrystEngComm* **2012**, *14*, 4738–4744. [CrossRef]
36. Leonyuk, N.I.; Leonyuk, L.I. Growth and characterization of $RM_3(BO_3)_4$ crystals. *Prog. Cryst. Growth Charact. Mater.* **1995**, *31*, 179–278. [CrossRef]
37. Sanjay; Kishore, N.; Agarwal, A. Investigation of structural, optical and transport properties of MoO_3–PbO–B_2O_3 glasses. *J. Alloys Compd.* **2009**, *487*, 52–57. [CrossRef]
38. Py1neva, N.A.; Kononova, N.G.; Yurkin, A.M.; Kokh, A.E.; Bazarova, G.G.; Danilov, V.I.; Lisova, I.A.; Tsirkina, N.L. Top-seeded solution growth of CLBO crystals. In Proceedings of the SPIE Conference on Laser Material Crystal Growth and Nonlinear Materials and Devices, San Jose, CA, USA, 27–28 January 1999.
39. Yu, X.S.; Hu, Z.G. Growth and characterization of Al-doped $CsLiB_6O_{10}$ crystal. *J. Cryst. Growth* **2011**, *318*, 1171–1174. [CrossRef]
40. Yu, X.S.; Hu, Z.G. Flux growth of $CsLiB_6O_{10}$ crystals. *J. Cryst. Growth* **2010**, *312*, 2415–2418. [CrossRef]
41. Kushwaha, S.K.; Rathee, S.P.; Maurya, K.K.; Bhagavannarayana, G. Enhancement in second harmonic generation efficiency, laser damage threshold and optical transparency of Mn^{2+} doped L-alanine crystals: A correlation with crystalline perfection. *J. Cryst. Growth* **2011**, *328*, 81–88. [CrossRef]
42. Li, X.M.; Hu, Z.G.; Yue, Y.C.; Yu, X.S.; Lin, Z.S.; Zhang, G.C. Study on optical weak absorption of borate crystals. *Opt. Mater.* **2013**, *35*, 2376–2381. [CrossRef]
43. Bhagavannarayana, G.; Kushwaha, S.K. Enhancement of SHG efficiency by urea doping in ZTS single crystals and its correlation with crystalline perfection as revealed by Kurtz powder and high-resolution X-ray diffraction methods. *J. Appl. Cryst.* **2010**, *43*, 154–162. [CrossRef]